Available online at www.sciencedirect.com
ScienceDirect
Acta Materialia 55 (2007) 6843–6851
Acta MATERIALIA
www.elsevier.com/locate/actamat

Predicting twinning stress in fcc metals: Linking twin-energy pathways to twin nucleation

S. Kibey [a], J.B. Liu [b], D.D. Johnson [a,b], H. Sehitoglu [a,*]

[a] University of Illinois at Urbana-Champaign, Department of Mechanical Science and Engineering, 1206 W. Green Street, Urbana, IL 61801, USA
[b] University of Illinois at Urbana-Champaign, Department of Materials Science and Engineering, 1304 W. Green Street, Urbana, IL 61801, USA

Received 31 July 2007; received in revised form 28 August 2007; accepted 30 August 2007
Available online 17 October 2007

Abstract

Deformation twinning is observed in numerous engineering and naturally occurring materials. However, a fundamental law for critical twinning stress has not yet emerged. We resolve this long-standing issue by integrating twin-energy pathways obtained via ab initio density functional theory with heterogeneous, dislocation-based twin nucleation models. Through a hierarchical theory, we establish an analytical expression that quantitatively predicts the critical twinning stress in face-centered cubic metals without any empiricism at any length scale. Our theory predicts a monotonic relation between the unstable twin stacking fault energy and twin nucleation stress revealing the physics of twinning.

Keywords: Twinning; Ab initio electron theory; Dislocation theory; Energy pathway

1. Introduction

Twinning is a predominant deformation mechanism in face-centered cubic (fcc) metals and alloys with low stacking fault energy (SFE). Twinning is also an important deformation mechanism in geological materials, body-centered cubic (bcc) and hexagonal closed-packed (hcp) metals. A fundamental understanding of the physics of twin activation is essential to capture the mechanical response of fcc materials. Since the earliest evidence of twinning in fcc metals [1,2,4,3,5–7], several efforts have been undertaken to incorporate twinning in order to predict their stress–strain response. In spite of these efforts, a long-standing issue remains unresolved, namely, predicting the critical stress (twinning stress) at which twinning initiates in fcc metals and alloys. Here, we establish a yield criterion for twinning in fcc metals by linking heterogeneous twin nucleation (described via mesoscale dislocation mechanics) and the twinning energy pathways (calculated via ab initio density functional theory).

It is now well accepted that twinning in metals and alloys is initiated by pre-existing dislocation configurations which dissociate into multi-layered stacking fault structures forming a twin nucleus. Several dislocation-based mechanisms [8–14] have been proposed to explain twin nucleation in fcc materials, although the dislocation configurations acting as a source of emanating twinning dislocations are different in each model. These mechanisms involve glide of Shockley partial dislocations (twinning dislocations with Burgers vector $|\mathbf{b}_{\text{twin}}| = a_0\langle 1\,1\,2\rangle/6$, where a_0 is the fcc lattice constant) on successive $\{1\,1\,1\}$ planes to create multi-layered faults that could then produce a twin. Fig. 1 shows the change of stacking in the fcc lattice due to passage of partial dislocations with Burgers vector $\mathbf{b}_{\text{p}} = \mathbf{b}_{\text{twin}}$, during twin nucleation. Passage of the partial on the first layer creates an intrinsic stacking fault (isf), and the second and third partials on successive planes then create a three-layer twin stacking fault (tsf). Passage of more partials on neighboring $\{1\,1\,1\}$ planes results in formation of larger twins. In

* Corresponding author. Tel.: +1 217 333 4112; fax: +1 217 244 6534.
E-mail address: huseyin@uiuc.edu (H. Sehitoglu).

1359-6454/$30.00
doi:10.1016/j.actamat.2007.08.042

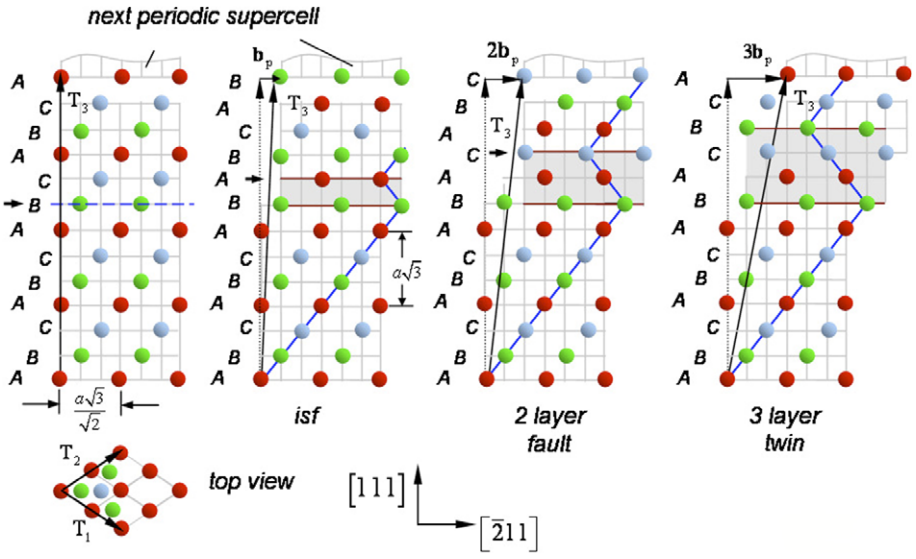

Fig. 1. The 12-layer supercell used for GPFE calculations: (from left to right) perfect fcc, one-layer (intrinsic) fault, two-layer fault and three-layer (twin) fault. The arrows indicate the successive {1 1 1} planes on which Shockley partials with Burgers vector $\mathbf{b}_p = a_0\langle 1\,1\,2\rangle/6$ are passed. The translation vector $\mathbf{T}_3$ maintains fcc stacking between adjacent supercells.

many of these models, the stress required to nucleate a twin has been determined from the stress required to operate a twin source such as a pileup, Lomer–Cottrell lock, etc. [9,12]. Typically, these models predict that the twinning stress depends only on the intrinsic stacking fault energy (SFE) γ_{isf} – for example, through a phenomenological relation of the form [12] $\tau_{crit} \sim K\gamma_{isf}/|\mathbf{b}_{twin}|$ with fitting parameter K to ensure good correlation with a limited range of experimental data. However, as shown recently, the energy pathways associated with twinning – the generalized planar fault energy (GPFE)–involve energy barriers which twinning partials must overcome during twin nucleation [15–17]; see Fig. 2a. The qualitative dependence of deformation twinning tendency on GPFE has been predicted in fcc metals [15,16,18] and alloys [17,19]. However, a quantitative dependence of twinning stress on GPFE has not been established yet; nor has the role of GPFE in classical dislocation-based, heterogeneous twinning stress models been accounted for. The twinnability approach [15,16], for example, provides only a qualitative measure of twinning propensity, namely, whether an fcc metal will twin or not. This approach does not address the twin nucleation issue, namely, at what stress an fcc metal will twin. The present work, on the other hand, provides a theory, free from adjustable parameters, that leads to a quantitative prediction of twinning stress.

In this paper, we incorporate the twin-energy pathways (GPFE) into a dislocation-based mechanistic model to predict the twinning stress in fcc metals (here for Ag, Al, Au, Cu, Ni, Pb, Pd and Pt). Of these, Al, Pd and Pt typically undergo cross-slip instead of twinning (Al has been reported to twin at crack tips [20] due to high stress concentration and is discussed later), while twinning in conventional Ni has been reported only at high stresses just prior to fracture [3,21]. As will be seen later, our model

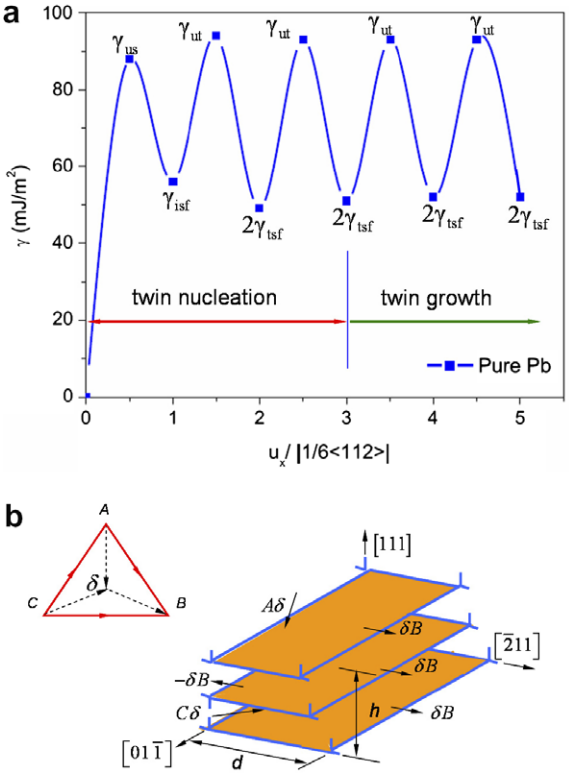

Fig. 2. (a) VASP–PAW GPFE for pure Pb vs. normalized shear displacement on successive {1 1 1} planes: twin-energy converges immediately after the third layer marking the start of twin growth. (b) The three-layer twin nucleus bounded by an array of partial dislocations (designated by Thompson tetrahedron in inset).

quantitatively predicts these differing deformation behaviors. Twinning has also been observed in nanocrystalline (10–50 nm grain size) Al [22,23] and Pd [24], but the observed twinning stresses are close to "ideal" stresses

(~1–2 GPa) [18], since the nanograins are almost dislocation-free and the observed twinning is attributed to emission of twinning partials from the grain boundaries. The present theory is for coarse-grained fcc metals, where twin nucleation in the bulk occurs without grain-boundaries as twin sources. In these fcc metals, pre-existing defects, such as stacking faults and fault pairs in the interior of the grain, act as twin nucleation sources, leading to twinning stresses that are an order of magnitude lower than the nearly ideal stresses in nanograined metals. Our theory reveals that the twinning stress in these fcc metals exhibits a more general dependence on the GPFE, rather than on a single parameter γ_{isf}. A natural outcome of our approach is that there are no adjustable parameters in our theory.

2. Hierarchical approach to twin nucleation

Here we model the deformation processes associated with twinning at two different length scales: (i) at the mesoscale level, where dislocations bounding the twin nucleus interact with each other; and (ii) at the atomic level, where lattice shears occurring due to passage of twinning partials involve traversing the twinning energy pathway (i.e. GPFE). We capture the mesoscale dislocation interactions using dislocation mechanics and use ab initio density functional theory (DFT) to determine the twinning energy pathway (GPFE) at the atomic level. We propose a sequential multi-scale model for twin nucleation that meaningfully incorporates the GPFE into a mesoscale dislocation-based mechanistic model. In the following section, we discuss the calculated twinning energy pathways (GPFE) for fcc metals and their importance in determining the twin nucleation event.

2.1. Twinning energy pathways

The GPFE provides a comprehensive description of twins [16,18,19,25,26]. For fcc systems, the GPFE is the energy per unit area required to form n-layer faults (twins) by shearing n successive $\{1\,1\,1\}$-layers along the $\langle 1\,1\,2\rangle$ direction – each through one Burgers vector of a Shockley partial $= |\mathbf{b}_{twin}| = a_0/\sqrt{6}$, see Fig. 1. The GPFE curves for fcc metals were determined with the Vienna ab initio simulation package [27,28] (VASP) using the generalized gradient approximation [29] (GGA) and the projector augmented wave [30] (PAW) basis. Fig. 1 shows a 12-layer supercell having 1-atom per layer with translation vectors $\mathbf{T}_1 = [1\,0\,\bar{1}]$, $\mathbf{T}_2 = [0\,1\,\bar{1}]$ and $\mathbf{T}_3$. We used periodic boundary conditions across the supercell to represent bulk fcc material (no free surfaces). Starting with the perfect fcc $\ldots ABC\ldots$ $(1\,1\,1)$-layer stacking, the intrinsic stacking fault was created by translating (sliding) layers 8–12 relative to layers 1–7 along $\mathbf{T}_3$ through one twinning partial Burgers vector $\mathbf{b}_{twin}$. We calculated the GPFE curves up to five-layer twins starting with a two-layer twin generated by sliding layers 9–12; then a three-layer twin by sliding layers 10–12, and so on. During shearing of the supercell, the vector $\mathbf{T}_3 = m|\mathbf{b}_{twin}| + n\,[1\,1\,1]$ (for m translations in an n-layer supercell) maintains fcc stacking between adjacent supercells, ensuring no unfavorable $\ldots AA\ldots$ configurations form in the stacking. All the atoms in the $\{1\,1\,1\}$-layers in the immediate vicinity of the fault, as well as the atoms in the layer containing the fault, were relaxed completely. The supercells are large enough to ensure convergence of the fault energies, i.e. defects are isolated. Brillouin zone sampling was performed using special k-point mesh [31] with the energy cutoffs 273.2 eV (Cu), 249.8 eV (Ag), 237.8 eV (Pb), 229.9 eV (Au), 240.4 eV (Al), 250.9 eV (Pd) and 230.3 eV (Pt), ensuring 1 meV atom^{-1} energy convergence.

Fig. 2a shows the predicted GPFE curve for Pb, as an example, where we define γ_{us} as the stacking fault nucleation barrier, γ_{isf} as the one-layer SFE, γ_{ut} as the twin nucleation barrier (unstable twin stacking fault energy) and $2\gamma_{tsf}$ as twice the twin SFE (or coherent twin boundary energy). Table 1 summarizes our calculated fault energies and their excellent agreement with experimental data. It is important to note that the experimental data for γ_{isf} and γ_{tsf} reported in the literature are based on various experimental techniques. There is some variability in the experimental data itself. For the majority of fcc metals (especially those which preferentially twin), the computed fault energies are within 5% of the experimentally reported value. Note also that energy barriers γ_{us} and γ_{ut} cannot be experimentally determined and must be computed. As will be seen later, twinning stress τ_{crit} for fcc metals strongly depends on the pathway barriers γ_{us} and γ_{ut}. Hence, we have calculated the entire GPFE curve (especially γ_{us} and γ_{ut}) using ab initio density functional theory. Our results may be compared with previous DFT [32,17,19,18] and more approximate, empirical methods [25,26,33,34] which lack sufficient accuracy. Table 1 represents the most complete group of DFT-based theoretical fault energy calculations for fcc metals.

Table 1
VASP–PAW–GGA fault energies (in mJ m^{-2}) for fcc metals (this study) at the experimental lattice constants (in parenthesis): intrinsic γ_{isf}; twin $2\gamma_{tsf}$; unstable intrinsic γ_{us}; and unstable twin γ_{ut}

Metal	γ_{us}	γ_{isf}		γ_{ut}	$2\gamma_{tsf}$	
	Theory	Theory	Expt.	Theory	Theory	Expt.[a]
Pb (4.95 Å)	87	49	–	92	44	–
Ag (4.09 Å)	133	18	16[a]	143	18	16
Au (4.08 Å)	134	33	32[a]	148	31	30
Cu (3.61 Å)	180	41	45[a]	200	40	48
Ni [b] (3.51 Å)	273	110	125[b]	324	110	86
Pd (3.89 Å)	287	168	180[b]	361	172	–
Pt (3.92 Å)	339	324	322[b]	486	321	322
Al (4.05 Å)	162	130	120[c]	215	113	150

Predicted values are in good agreement with experiment. Metals that twin are in bold. Dash indicates that experimental data were not available for comparison.

[a] Fault energies from Table A-1 of Ref. [35].

[b] Fault energies from Ref. [19].

[c] Ref. [56].

From Fig. 2a, we note that $2\gamma_{tsf}$ converges after third layer sliding for pure Pb. We have observed similar convergence trends in pure Cu and Cu–Al alloys [17], as well as in all fcc metals investigated here (shown in bold in Table 1) that undergo twinning. In fcc metals, the fault energies continue to vary until the third layer has nucleated. Beyond the third layer, the fault energies converge immediately with nucleation of subsequent layers. The three-layer fault is the smallest possible twin in fcc metals [35,36], and is commensurate with the Mahajan–Chin model [13]. We note that a previous study [18] reported convergence for pure Cu at two-layers based on a slab geometry in vacuum, which is in contrast to our periodic supercells that maintain bulk environment. This difference in boundary conditions may explain the difference in GPFE convergence behavior. The present results also suggest that, in fcc metals and alloys, the formation of a three-layers-thick twin is best described as the *twin nucleation event* (see Fig. 2a). Any further increase in the twin thickness must be described as a *twin growth event*, where fault energies remain unchanged with increasing twin thickness.

Most previously reported GPFE results for fcc metals were computed using either empirical potential-based methods [15,16,25,26,33,34,37] or DFT [19] for two-layer defects only. However, a GPFE calculation for up to only two-layers is insufficient to study the energy of twin nucleation, where the smallest twin is commensurate with three-layers [35,36]. The distinction between twin nucleation and twin growth is important as the stress required for twin growth is much less than that required for nucleation [9,38,39]. The correct prediction of twin nucleation stress requires a heterogeneous, dislocation-based mesoscale model and is described next.

2.2. Dislocation-based mesoscale model

To determine the twinning stress, one may consider the equilibrium of forces acting on individual dislocations bounding the twin nucleus [9,12,38–41]. Alternatively, it is possible to determine the twinning stress by considering the total energy associated with the dislocation configuration forming the twin and differentiating the total energy with respect to twin width d and height h. In this work, we calculate the total energy for a twin nucleus along with its bounding partials. While several dislocation configurations bounding the twin nucleus have been proposed [8,9,11,13,14], here we consider the three-layer twin nucleus proposed by Mahajan and Chin [13] (see Fig. 2b). Since the twin nucleus is very thin, the dislocations are treated as coplanar, in accordance with Friedel [42]. As will be seen, this twin configuration is adequate to capture the energetics of twin nucleation with excellent accuracy.

Fig. 2b shows the three-layer twin nucleus along with its bounding partial dislocations. Since the three bounding partial dislocations on the left have a zero net Burgers vector, these partials are immobile and will not participate in the widening of the twin nucleus. Only the mobile $\delta\mathbf{B}$ twinning partial dislocations will cause widening of the twin nucleus within the volume of the grain. Further, thickening of the twin nucleus will occur due to the combination and agglomeration of these three-layer twin nuclei, as postulated by Mahajan and Chin [13]. Since we are interested in determining the true (as opposed to the "ideal") twinning stress (the critical shear stress required to nucleate a twin in an fcc crystal), we focus on the energetics associated with the three-layer twin nucleus configuration shown in Fig. 2b.[1]

The total energy of the three-layer twin nucleus shown in Fig. 2b is composed of: (i) the elastic energy of edge and screw components of dislocations bounding the nucleus, (ii) work done by applied resolved shear stress and (iii) the energy associated with the twinning energy pathway GPFE (i.e. the area under the GPFE curve). From Fig. 2b, it is seen that, of all the bounding partial dislocations, only $\mathbf{A}\delta$ and $\mathbf{C}\delta$ have mixed character. The remaining $\delta\mathbf{B}$ twinning partials are pure edge partial dislocations. This property allows us to determine the total elastic energy associated with the dislocation configuration using well-established closed-form expressions for dislocation walls and pileups. The total energy can be expressed as:

$$E_{\text{total}} = E_{\text{edge}} + E_{\text{screw}} - W_{\tau} + E_{\text{GPFE}} \tag{1}$$

Since, the twin nucleus is only three-layers thick, we consider the twin to be thin, allowing us to treat the edge components of the partial dislocations as a single pileup in accordance with Friedel [42]. Following classical dislocation theory for pileups [44], the elastic energy associated with the edge components can be written as:

$$E_{\text{edge}} = \frac{G_{\{1\,1\,1\}}}{4\pi(1-\nu)}|\mathbf{b}_e|^2 d\left[N^2\left\{\ln\left(\frac{d}{N}\right)+\frac{1}{2}\right\} - N\ln\left(\frac{d}{w}\right) - \frac{1}{6}\ln(N)\right] \tag{2}$$

where $\mathbf{b}_e$ is the Burgers vector of the edge component of the partial, d is the width of the twin nucleus, w is the core width and N is the number of $\{1\,1\,1\}$-layers in the twin nucleus (equal to 3, as already established from our first principles calculations).

Further, as only $\mathbf{A}\delta$ and $\mathbf{C}\delta$ are mixed dislocations, the screw components can be treated as a finite sized vertical wall [45] and their elastic energy contribution can be expressed as:

[1] We can alternatively consider the twin nucleus as a helical dislocation configuration with varying radius (similar to a pole mechanism). De Wit [43] has developed closed-form elasticity solutions for a uniform radius helical dislocation configuration. However, these elasticity solutions apply only to the limiting cases of very small and large radii dislocation helixes. These solutions, while attractive, are not applicable to the helical partial dislocation in the pole mechanism, for example. In the present theory, we use classical elasticity solutions for the three-layer twin nucleus proposed by Mahajan and Chin [13] and show that the derived closed-form expressions are more than adequate to capture the energetics of twin nucleation with excellent accuracy.

$$E_{\text{screw}} = \frac{G_{\{1\,1\,1\}}}{9\pi}\left|\mathbf{b}_s\right|^2 d\,N^2\left[\ln\left(\frac{d}{N}\right) - \frac{1}{2}\right] \tag{3}$$

The energy contribution E_{GPFE} of the GPFE curve can be divided into two parts: $E_{\gamma\text{-twin}}$, the energy required to nucleate the twin, and $E_{\gamma\text{-SF}}$, the energy required to create an intrinsic stacking fault

$$E_{\text{GPFE}} = E_{\gamma-\text{twin}} - E_{\gamma-\text{SF}} \tag{4}$$

The above additive decomposition of E_{GPFE} arises because cross-slip and twinning are competing mechanisms and are controlled by different regions of the GPFE curve. In order to identify $E_{\gamma\text{-SF}}$ and $E_{\gamma\text{-twin}}$ in a physically meaningful way, we express the GPFE curve in Fig. 2a as

$$\begin{aligned}
&\gamma(\lambda(x)) = \gamma_{\text{SF}}(\lambda(x)) + \gamma_{\text{twin}}(\lambda(x)), \quad \lambda(x) = \frac{u_x}{|\mathbf{b}_{\text{twin}}|}\\
&\gamma_{\text{SF}}(\lambda(x)) = f(\gamma_{\text{us}},\ \gamma_{\text{isf}}) \quad \text{for } 0 \leqslant \lambda(x) \leqslant 1\\
&\gamma_{\text{twin}}(\lambda(x)) = g(\gamma_{\text{isf}},\ \gamma_{\text{ut}}, \gamma_{\text{tsf}}) \quad \text{for } 0 \leqslant \lambda(x) < N
\end{aligned} \tag{5}$$

In the above equation, $\lambda(x) = u_x/|\mathbf{b}_{\text{twin}}|$ is the normalized relative shear displacement that the two halves of the crystal undergo due passage of a Shockley partial. The energy contributions of $E_{\gamma\text{-SF}}$ and $E_{\gamma\text{-twin}}$ can be expressed as follows:

$$\begin{aligned}
E_{\gamma-\text{twin}} &= (N-1)\ d\int_0^d \gamma_{\text{twin}}\ \mathrm{d}x\\
E_{\gamma-\text{SF}} &= d\int_0^d \gamma_{\text{SF}}\ \mathrm{d}x
\end{aligned} \tag{6}$$

From Eq. (6), the area under the $\gamma_{\text{SF}}(\lambda(x))$ curve is the energy $E_{\gamma\text{-SF}}$ required to overcome the unstable stacking fault energy barrier γ_{us} and nucleate an intrinsic stacking fault in the lattice. Further, as already discussed in a previous paper [32], $E_{\gamma\text{-SF}}$ is also a measure of the energy required to recombine the partials during cross-slip at the onset of stage III hardening. Since twinning and cross-slip are competing mechanisms, $E_{\gamma\text{-SF}}$ will not assist in twin formation. This is accounted for by the negative sign in front of $E_{\gamma\text{-SF}}$ in the total energy Eq. (4). On the other hand, the area under the $\gamma_{\text{twin}}(\lambda(x))$ curve is the energy $E_{\gamma\text{-twin}}$ (see Eq. 6) required by the twinning partials $\delta\mathbf{B}$ to overcome the twin nucleation barrier γ_{ut} during the nucleation of the three-layer twin. The twin nucleation barrier γ_{ut} can be split into its constituent twin energies as follows [18]:

$$\gamma_{\text{ut}} = 2\gamma_{\text{TBF}} + \gamma_{\text{TBM}}$$

where $2\gamma_{\text{TBF}}$ is the twin boundary formation energy (equal to the coherent twin boundary energy [46]) or the twin stacking fault energy, i.e. $2\gamma_{\text{TBF}} = 2\gamma_{\text{tsf}}$) and γ_{TBM} is the twin boundary migration energy. The passage of Shockley partials over successive $\{1\,1\,1\}$ planes results in propagation of the twin boundary front in the $\langle 1\,1\,1\rangle$ direction normal to the K_1 plane. In order to migrate the twin boundary to the next $\{1\,1\,1\}$ plane, the partial must have enough energy to overcome the γ_{TBM} barrier. Once the barrier is overcome, the twin attains a stable configuration with a stable energy equal to $2\gamma_{\text{TBF}}$ or $2\gamma_{\text{tsf}}$. We account for both twin boundary migration and formation energies through the energy term $E_{\gamma\text{-twin}}$ in Eq. (4).

To determine the energy contributions $E_{\gamma\text{-SF}}$ and $E_{\gamma\text{-twin}}$ from Eq. (6), we follow the classical Peierls model [47] for periodic lattices: the function $f(\gamma_{\text{us}}, \gamma_{\text{isf}})$ (GSFE for a stacking fault) in Eq. (5) has been expressed as a cosine function of the fault energies [35,48]. Here, we use the cosine analytical form for both f and g in Eq. (5) to express γ_{SF} and γ_{twin} as follows:

$$\begin{aligned}
\gamma_{\text{SF}}(\lambda(x)) &= \left(\frac{\gamma_{\text{us}} + \gamma_{\text{isf}}}{2}\right) - \left(\frac{\gamma_{\text{us}} - \gamma_{\text{isf}}}{2}\right)\cos\left(2\pi\lambda(x)\right)\\
\gamma_{\text{twin}}(\lambda(x)) &= \frac{1}{2}\left[\gamma_{\text{ut}} + \left(\frac{2\gamma_{\text{tsf}} + \gamma_{\text{isf}}}{2}\right)\right]\\
&\quad - \frac{1}{2}\left[\gamma_{\text{ut}} - \left(\frac{2\gamma_{\text{tsf}} + \gamma_{\text{isf}}}{2}\right)\right]\cos\left(2\pi\lambda(x)\right)
\end{aligned}$$

The applied shear stress τ resolved on the appropriate twin system (e.g. in the $[\bar{2}\,1\,1]$ direction in Fig. 2b) assists the leading Shockley partials $\delta\mathbf{B}$ to break away from the immobile trailing partials on the left. Thus, the shear stress τ helps to overcome the twinning barrier γ_{ut} and the work W_τ done in displacing the twinning partials through width d is given by

$$W_\tau = N\tau|\mathbf{b}_{\text{twin}}|d^2 \tag{7}$$

Having determined all the terms in the total energy expression, the total energy of the twin nucleus shown in Fig. 2b can be written as follows:

$$\begin{aligned}
E_{\text{total}} = \frac{G_{\{1\,1\,1\}}}{4\pi(1-\nu)}|\mathbf{b}_e|^2\ d\left[N^2\left\{\ln\left(\frac{d}{N}\right) + \frac{1}{2}\right\} - N\ln\left(\frac{d}{w}\right)\right.\\
\left. - \frac{1}{6}\ln(N)\right] + \frac{G_{\{1\,1\,1\}}}{9\pi}|\mathbf{b}_s|^2\ d\ N^2\left[\ln\left(\frac{d}{N}\right) - \frac{1}{2}\right]\\
+ (N-1)\ d\int_0^d \gamma_{\text{twin}}\ \mathrm{d}x - d\int_0^d \gamma_{\text{SF}}\ \mathrm{d}x - N\tau|\mathbf{b}_{\text{twin}}|d^2
\end{aligned} \tag{8}$$

where $G_{\{1\,1\,1\}}$ is the shear modulus on the activated $\{1\,1\,1\}$ plane and w is the core radius. The shear modulus $G_{\{1\,1\,1\}}$ of a cubic crystal was determined for each fcc metal from its elastic moduli C_{11}, C_{12} and C_{44} using the following equation [49]:

$$G_{\{1\,1\,1\}} = \frac{3C_{44}(C_{11} - C_{12})}{4C_{44} + C_{11} + C_{12}} \tag{9}$$

Table 2 summarizes the elastic moduli [50,51] and the calculated shear modulus $G_{\{1\,1\,1\}}$ for each metal investigated here. Note from Eq. (8) that the total energy E_{total} depends only on (i) the geometry of the twin nucleus (twin width d, dislocation core width w and the number of layers N) and (ii) the fault energies γ_{isf}, $2\gamma_{\text{tsf}}$, γ_{us} and γ_{ut}, which are determined from first principles. Note that the energies in Eq. (8) are insensitive to temperature changes and so will be the twinning stress, in agreement with experiments. To determine the twinning stress τ_{crit}, we minimized the total energy of the three-layer nucleus with respect to d

Table 2
Summary of the lattice constants, elastic moduli and the computed shear modulus $G_{\{1\,1\,1\}}$ for fcc metals

Metal	a_0 (Å)	C_{11} (GPa)	C_{12} (GPa)	C_{44} (GPa)	$G_{\{1\,1\,1\}}$ (GPa)
Pb[a]	4.95	55.6	45.4	19.4	3
Ag[a]	4.16	131.5	97.3	51.1	12
Au[a]	4.08	201	170	46	8
Cu[b]	3.61	225	153	115	30
Ni[a]	3.52	261	151	132	46
Al[a]	4.05	114	62	32	16
Pd[a]	3.89	234	176	71.2	18
Pt[a]	3.92	358	253	77.5	27

The elastic moduli C_{11}, C_{rm12} and C_{44} have been used from experimental data or from first principles calculations.
[a] Elastic moduli C_{ij} from Ref. [50].
[b] Elastic moduli C_{ij} from Ref. [51].

$\left(\text{i.e. } \frac{\partial E_{\text{total}}}{\partial d} = 0\right)$ and N $\left(\text{i.e. } \frac{\partial E_{\text{total}}}{\partial N} = 0\right)$ and derived an explicit, closed-form expression for $\tau = \tau(\gamma_{\text{isf}}, \gamma_{\text{tsf}}, \gamma_{\text{us}}, \gamma_{\text{ut}}, G_{\{1\,1\,1\}}, N, d)$ given by

$$\begin{aligned}\tau(d) = {} & \frac{G_{\{1\,1\,1\}}N}{\pi d}\left[\frac{|\mathbf{b}_{\text{e}}|^2}{4(1-\nu)} + \frac{|\mathbf{b}_{\text{s}}|^2}{9}\right] \\ & + \frac{2}{3N|\mathbf{b}_{\text{twin}}|}\left(\frac{3N}{4} - 1\right)\left[\gamma_{\text{ut}} + \frac{(2\gamma_{\text{tsf}} + \gamma_{\text{isf}})}{2}\right] \\ & - \frac{2}{3N|\mathbf{b}_{\text{twin}}|}(\gamma_{\text{ut}} + \gamma_{\text{isf}}) + \frac{1}{6|\mathbf{b}_{\text{twin}}|}\left[\gamma_{\text{ut}} - \frac{(2\gamma_{\text{tsf}} + \gamma_{\text{isf}})}{2}\right]\left(\frac{w}{d}\right) \\ & \times \left[\ln\left(\frac{d + \sqrt{d^2 + w^2}}{w}\right)\right] \\ & - \frac{(N-1)}{3N}\left[\gamma_{\text{ut}} - \frac{(2\gamma_{\text{tsf}} + \gamma_{\text{isf}})}{2}\right]\left(\frac{w}{d}\right) \\ & \times \left[\ln\left(\frac{d + \sqrt{d^2 + w^2}}{w}\right) + \frac{d}{\sqrt{d^2 + w^2}}\right] \\ & + \frac{1}{3N|\mathbf{b}_{\text{twin}}|}(\gamma_{\text{us}} - \gamma_{\text{isf}})\left(\frac{w}{d}\right) \\ & \times \left[\ln\left(\frac{d + \sqrt{d^2 + w^2}}{w}\right) + \frac{d}{\sqrt{d^2 + w^2}}\right] \end{aligned} \tag{10}$$

Note that, for a given fcc crystal, the only unknowns in Eq. (10) are τ and d. The above $\tau(d)$ equation was solved numerically for τ_{crit} and d using mathematica. To determine τ_{crit} we impose a geometric constraint on the above equation: for nucleation of a stable twin, its width d must be at least equal to the Burgers vector of the twinning dislocation, i.e. $d \geqslant |\mathbf{b}_{\text{twin}}|$. In other words

$$\tau_{\text{crit}} = \begin{cases} \text{Minimize} & \tau(d) \\ \text{subject to} & d \geqslant |\mathbf{b}_{\text{twin}}| \end{cases}$$

Eq. 10 reveals that $\tau(d)$ and, hence, the twinning stress τ_{crit} depends on the fault energies (γ_{isf}, γ_{tsf}, γ_{us} and γ_{ut}) and geometric parameters N (equal to 3 for fcc twin nucleus, as discussed before), w (equal to $0.2|\mathbf{b}_{\text{twin}}|$ for pure metals [35]) and twin width d. The choice of w has minimal impact on our results. Thus, no adjustable parameters are present in the twinning stress equation arising from either DFT or mesoscale dislocation theory. All parameters are quantities intrinsic to the fcc metals under consideration. Further, note that, since the fault energies vary weakly with temperature, our theory predicts that twinning stress is insensitive to temperature, in agreement with observations [38,52].

3. Results and discussion

Fig. 3 shows the predicted width d and aspect ratio h/d of the twin nucleus plotted against the predicted twinning stress. The plot represents (τ, d) values that satisfy the objective function $\tau(d)$ and the inequality constraint $d \geqslant |\mathbf{b}_{\text{twin}}|$. Our theory predicts that the nucleating deformation twins will be of lenticular morphology (small h/d ratio), in agreement with experiments and classical nucleation theory [53]. During twin growth, the width d will be limited by the grain size. Further, it is seen that the metals with higher twinning stress will accommodate thinner twin nuclei.

In Table 3 and Fig. 4, we compare the twinning stress predicted from our DFT-based analytic theory with the experimental twinning stress data, and find excellent agreement without any fitting parameters at any length scale. Also included in Table 3 is the oft-quoted "ideal twinning stress" determined from the derivative of GPFE [18] ($\tau_{\text{ideal}} = \pi(\gamma_{\text{ut}} - 2\gamma_{\text{tsf}})/|\mathbf{b}_{\text{twin}}|$), which is an order of magnitude larger than the true nucleation stress for twinning observed experimentally. Fig. 4a shows a non-monotonic relationship between τ_{crit} and γ_{isf}, which cannot be explained by the classical twinning models [9,10,12,54] that proposed a monotonic (either linear or quadratic) relationship between these two quantities. However, our hierarchical approach captures the observed non-monotonic trend accurately. More importantly, our twinning stress equation reveals that τ_{crit} is determined from the entire GPFE (γ_{isf}, γ_{us}, γ_{tsf} and γ_{ut}) and not just γ_{isf}, as suggested by classical phenomenological models.

Our theory, for the first time, establishes an extremely important correlation between τ_{crit} and γ_{ut} in fcc metals. In Fig. 4b, we plot the predicted and experimental twinning stress of all fcc metals considered here against γ_{ut}. Fig. 4b shows a monotonic increase in twinning stress with γ_{ut}, which classical phenomenological models cannot capture.

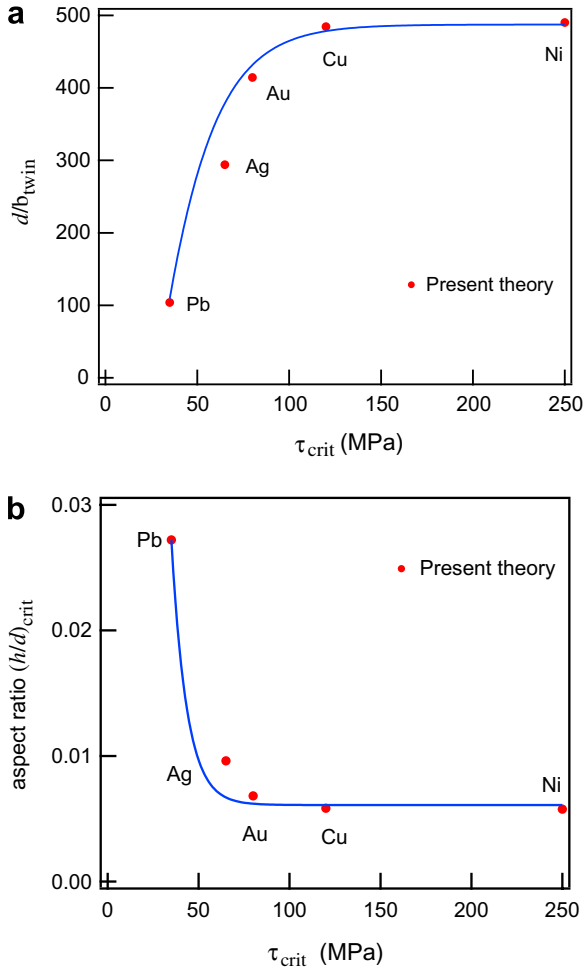

Fig. 3. Predicted twin nucleus size (circles): (a) twin width d normalized by twinning partial Burgers vector vs. predicted twinning stress. The theory predicts that fcc metals with higher twin nucleation stress will accommodate wider twin nuclei. (b) Predicted twin aspect ratio vs. twinning stress (h is the twin thickness). The line is a guide to the eye. Note that fcc metals with higher twin nucleation stress will accommodate twin nuclei with smaller aspect ratios.

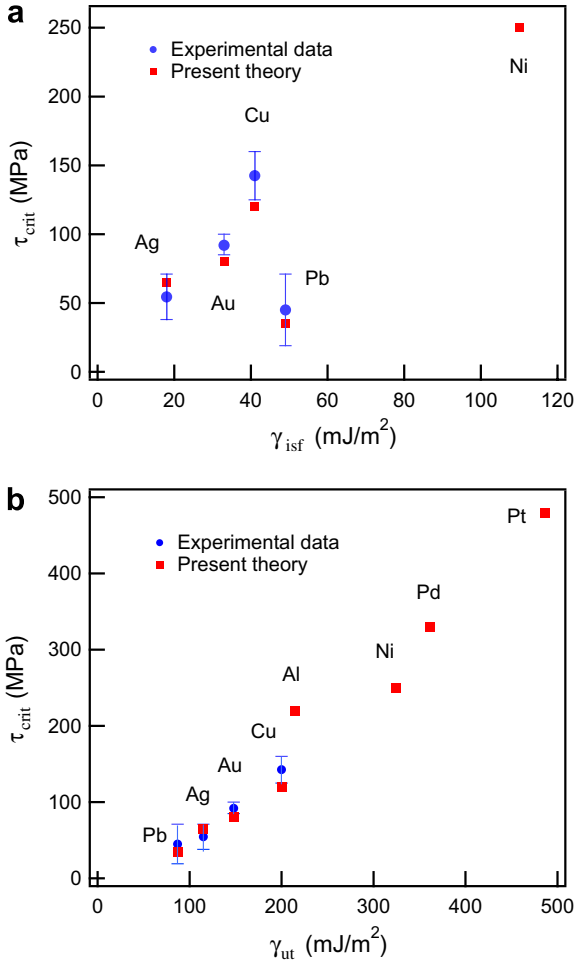

Fig. 4. From Table 3, predicted and experimental twinning stress for fcc metals vs. GPFE: (a) intrinsic SFE γ_{isf} and (b) unstable twin SFE, γ_{ut}. The predicted twinning stress (square) is in excellent agreement with the experimental data (circles). Our theory captures the non-monotonic dependence of twinning stress on γ_{isf} with excellent accuracy. The theory also reveals a monotonic trend between τ_{crit} and γ_{ut}, thus suggesting that γ_{ut} is a critical fcc material property governing twin nucleation.

Table 3
Predicted critical twinning stress τ_{crit}^{theory} and "ideal" twinning stresses τ_{ideal}^{theory} (MPa) for fcc metals (present work), compared with known reported experimental values (from literature) τ_{crit}^{expt}

Metal	τ_{crit}^{theory} (MPa) (predicted)	τ_{crit}^{expt} (MPa) (expt.)	τ_{ideal}^{theory} (MPa)	Deformation mechanism
Pb	40	19–71[a]	660	Twinning
Ag	65	38–71[b]	1910	Twinning
Au	80	85–100[c]	2210	Twinning
Cu	120	125–160[d]	3380	Twinning
Ni	250	–	4680	Twinning
Al	220	–	1940	Cross-slip
Pd	330	–	5260	Cross-slip
Pt	480	–	3240	Cross-slip

The theory provides quantitative agreement to experiment and correctly predicts the dominant deformation mechanism (twinning vs. cross-slip). Dash indicates that experimental data was not available for comparison.

[a] Ref. [7].
[b] Ref. [2,55].
[c] Ref. [55].
[d] Ref. [57].

The physics can be explained as follows: γ_{ut} is the sum of the twin boundary migration energy and the twin boundary formation energy [18]. In other words, to form a twin boundary and translate it onto the next {1 1 1} plane during twin nucleation, the Shockley partial must overcome the barrier γ_{ut}. The higher the γ_{ut} barrier, the larger the stress required to overcome it and allow passage of Shockley partial to the successive {1 1 1} plane. Consequently, fcc metals with larger twin nucleation barriers γ_{ut} exhibit larger twinning stress – a trend confirmed by both experimental data and present theory (see Fig. 4b). The present work also highlights the role of unstable SFE γ_{us}. We have recently shown that the unstable stacking fault energy governs the intrinsic stacking fault width and, therefore, the energy needed to recombine the partials during cross-slip [32]. Thus, an increase in γ_{us} inhibits cross-slip and promotes twinning. For completeness, it is worth noting that ad hoc twinning stress relations, such as $(\tau_{crit} = \gamma_{isf}/2|\mathbf{b}_{twin}|)$, do not predict the correct twinning stress for all fcc metals, while our hierarchical, adjustable parameter-free approach does.

Our theory also resolves an apparent contradiction from experiments regarding observed twinning in conventional pure Ni. Haasen and King [3] and Robertson [21] have reported twinning in Ni at high stresses just prior to fracture (tensile strength of Ni is 317 MPa), but they did not report a twinning stress. We predict that twinning in Ni will occur (if at all) at 250 MPa due to its very high twin nucleation barrier γ_{ut}. Narita and colleagues [55] did not observe twinning in Ni, since their applied shear stresses were lower than this critical value.

Coarse-grained Al has not been experimentally observed to deform by twinning, except at crack tips [20] – most likely due to very high stress concentration. This has been typically attributed to the high intrinsic SFE of Al. Table 1 shows that while γ_{ut} for Al is only slightly higher than that for Cu, its γ_{isf} and γ_{tsf} are almost three times larger than the corresponding energies for pure Cu. Additionally, the cross-slip barrier γ_{us} for Al is much lower than that for Cu, thus making cross-slip more favorable than twinning in Al. Also, twinning as a deformation mechanism has not been observed in conventional Pd and Pt. As seen in Table 1, both Pd and Pt have a very high unstable twin nucleation barrier γ_{ut} (1.8 and 4 times larger than Cu for Pd and Pt, respectively) that well exceeds the corresponding cross-slip barrier γ_{us}. Consequently, our theory suggests a very high value of twinning stress for Pd (330 MPa) and Pt (480 MPa), indicating that these metals will preferentially undergo cross-slip at the onset of stage III hardening and not necessarily deform by twining.

4. Conclusion

We have presented a hierarchical, multi-scale theory that links the lattice shears at the atomic scale to the dislocation interactions at the mesoscale captured via heterogeneous twin nucleation models. The theory suggests a dependence of the true twinning stress τ_{crit} on the entire generalized planar fault energy, not just on the intrinsic stacking fault energy γ_{isf} suggested by classical phenomenological models. Moreover, our theory reveals the underlying physics of twin nucleation in fcc metals – namely, twinning stress has a non-monotonic dependence on intrinsic stacking fault energy which classical models fail to explain, but bears a monotonic dependence on the unstable twin stacking fault energy γ_{ut} (also borne out with experimental data). Our first-principles-based theory permits, for the first time, a quantitative prediction of the twinning stress for fcc metals that is in excellent agreement with experiments without requiring any adjustable parameters at any length scale.

Acknowledgements

National Science Foundation supported this research mainly under Grants DMR-03-13489 and DMR-03-12448, with additional support under DMR-01-21695 and computational support from the Materials Computational Center under DMR-03-25939.

References

[1] Blewitt TH, Coltman RR, Redman JK. J App Phys 1957;28:651.
[2] Suzuki H, Barrett CS. Acta Metall 1958;6:156.
[3] Haasen P, King A. Z Metallkd 1960;51:722.
[4] Haasen P. Philos Mag 1958;3:384.
[5] Thornton PR, Mitchell TE. Philos Mag 1962;7:361.
[6] Armstrong RW. In: Reed-Hill RE, Hirth JP, Rogers HC, editors. Deformation twinning. New York: Gordon & Breach; 1964. p. 356.
[7] Bolling GF, Casey KW, Richman RH. Philos Mag 1965;12:1079.
[8] Cohen JB, Weertman J. Acta Metall 1963;11:996.
[9] Venables JA. In: Reed-Hill RE, Hirth JP, Rogers HC, editors. Deformation twinning. New York: Gordon & Breach; 1964. p. 77.
[10] Venables JA. J Phys Chem Solids 1964;25:685.
[11] Hirth JP. In: Reed-Hill RE, Hirth JP, Rogers HC, editors. Deformation twinning. New York: Gordon & Breach; 1964. p. 112.
[12] Muira S, Takamura J-I, Narita N. Trans J Inst Met Suppl 1968;9:S555.
[13] Mahajan S, Chin GY. Acta Metall 1973;21:1353.
[14] Fujita H, Mori T. Scripta Metall 1975;9:631.
[15] Bernstein N, Tadmor EB. Phys Rev B 2004;69:094116.
[16] Tadmor EB, Bernstein N. J Mech Phys Solids 2004;52:2507.
[17] Kibey S, Liu J-B, Johnson DD, Sehitolgu H. Appl Phys Lett 2006;89:191911.
[18] Ogata S, Li J, Yip S. Phys Rev B 2005;71:224102.
[19] Siegel DJ. Appl Phys Lett 2005;87:121901.
[20] Pond RC, Garcia-Garcia LMF. In: Electron Microscopy and Analysis, 1981. Proceedings of the Institute of Physics Electron Microscopy and Analysis Group Conference. IOP, Cambridge, 1982.
[21] Robertson IM. Philos Mag A 1986;54:821.
[22] Chen M, Ma E, Hemker KJ, Sheng H, Wang Y, Cheng X. Science 2003;300:1275.
[23] Zhu YT, Liao XZ, Srinivasan SG, Zhao YH, Baskes MI, Zhou EJ, et al. Appl Phys Lett 2004;85:5049.
[24] Rosner H, Markmann J, Weissmuller J. Philos Mag Lett 2004;84:321.
[25] Van Swygenhoven H, Derlet PM, Froseth AG. Nature Mater 2004;3:399.
[26] Froseth AG, Derlet PM, Van Swygenhoven H. Appl Phys Lett 2004;85:5863.
[27] Kresse G, Hafner J. Phys Rev B 1993;47:558.

[28] Kresse G, Furthmuller J. Phys Rev B 1996;54:11169.
[29] Perdew J, Wang Y. Phys Rev B 1992;45:13244.
[30] Kresse G, Joubert D. Phys Rev B 1999;59:1758.
[31] Monkhorst HJ, Pack JD. Phys Rev B 1976;13:5188.
[32] Kibey S, Liu JB, Curtis MJ, Johnson DD, Sehitoglu H. Acta Mater 2006;54:2991.
[33] Zimmerman JA, Gao H, Abraham FF. Model Simul Mater Sci Eng 2000;8:103.
[34] Mehl MJ, Papaconstantopoulos DA, Kioussis N, Herbranson M. Phys Rev B 2000;61:4894.
[35] Hirth JP, Lothe J. Theory of dislocations. 2nd ed. New York: Wiley-Interscience; 1982.
[36] Nabarro FRN. Theory of crystal dislocations. Oxford: Oxford University Press; 1967.
[37] Szelestey P, Patriarca M, Perondi LF, Kaski K. Int J Mod Phys B 2002;16:2823.
[38] Christian JW, Mahajan S. Prog Mater Sci 1995;39:1.
[39] Christian JW. The theory of transformations in metals and alloys. 3rd ed. New York: Pergamon Press; 2002.
[40] Cooper RE. Acta Metall 1965;13:46.
[41] Cooper RE. Acta Metall 1966;14:78.
[42] Friedel J. Dislocations. 3rd ed. Reading, MA: Addison-Wesley; 2002.
[43] De Wit R. Phys Rev 1959;116:592.
[44] Chou YT, Li JCM. Theory of dislocation pileups. In: Mura T, editor. Mathematical theory of dislocations. Evanston, IL: Springer; 1969.
[45] Li JCM. Acta Metall 1960;8:563.
[46] Murr LE. Interfacial phenomena in metals and alloys. Reading, MA: Addison-Wesley; 1975.
[47] Peierls RE. Proc Phys Soc Lond 1940;52:34.
[48] Rice JR. J Mech Phys Solids 1992;40:239.
[49] Roundy D, Krenn CR, Cohen ML, Morris Jr JW. Phys Rev Lett 1999;82:2713.
[50] Simmons G, Wang H. Single crystal elastic constants and calculated aggregate properties: a handbook. Cambridge, MA: MIT; 1971.
[51] Jona F, Marcus PM. Phys Rev B 2001;63:094113.
[52] Meyers MA, Benson DJ, Vohringer O, Kad BK, Xue Q, Fu HH. Mater Sci Eng A 2002;322:194.
[53] Christian JW. Acta Metall 1958;6:377.
[54] Meyers MA, Vohringer O, Lubarda VA. Acta Metall 2001;49:4025.
[55] Narita N, Hatano A, Takamura J, Yoshida M, Sakamoto H. J Jpn Inst Met 1978;42:533.
[56] Rautioaho RH. Phys Stat Solid B 1982;112:83.
[57] Yamamoto A, Narita N, Takamura J, Sakamoto H, Matsuo N. J Jpn Inst Met 1983;47:903.